

Multimodal-based Scene-Aware Framework for Aquatic Animal Segmentation

Minh-Quan Le^{1,5}, Trung-Nghia Le², Tam V. Nguyen³, Isao Echizen², and Minh-Triet Tran^{1,4,5}

¹University of Science, Ho Chi Minh City, Vietnam

²National Institute of Informatics, Japan

³University of Dayton, US

⁴John von Neumann Institute, VNU-HCM, Vietnam

⁵Vietnam National University, Ho Chi Minh City, Vietnam

December 14, 2021

Abstract

Recent years have witnessed great advances in object segmentation research. In addition to generic objects, aquatic animals have attracted research attention. Deep learning-based methods are widely used for aquatic animal segmentation and have achieved promising performance. However, there is a lack of challenging datasets for benchmarking. Therefore, we have created a new dataset dubbed “Aquatic Animal Species.” Furthermore, we devised a novel multimodal-based scene-aware segmentation framework that leverages the advantages of multiple view segmentation models to segment images of aquatic animals effectively. To improve training performance, we developed a guided mixup augmentation method. Extensive experiments comparing the performance of the proposed framework with state-of-the-art instance segmentation methods demonstrated that our method is effective and that it significantly outperforms existing methods.

1 Introduction

Computer vision is an interdisciplinary research field that helps computers gain understanding from images and videos. The rapid development of deep learning tech-

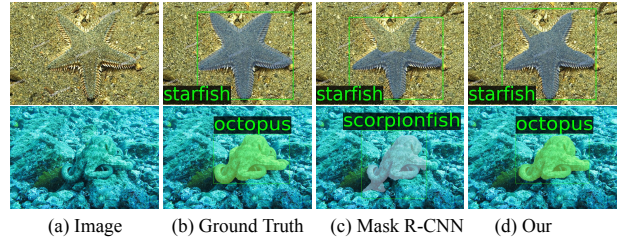


Figure 1: Visual comparison of our method with baseline model.

niques has enabled computer vision applications to become a part of daily life, such as autonomous driving, medical treatment, and entertainment. These applications require detection and segmentation of various types of objects appearing in images and videos [1, 2].

Animal-related research has recently drawn the attention of the computer vision community. As a result, the number of studies involving animal research using computer vision and deep learning techniques has been increasing. Examples include measurement of animal behavior [3] and analysis of animal trajectories [4]. In addition, various animal-related datasets have been constructed for specific research purposes [5–7]. However, there is a lack of research on aquatic animals, especially on automatically localizing and recognizing aquatic ani-

imals. We attribute this partially to the lack of appropriate datasets for training, testing, and benchmarking. It has thus become essential to develop methods for aquatic animal instance segmentation.

To encourage more studies on aquatic animal segmentation, we have created a dataset we call “Aquatic Animal Species (AAS).” It consists of 4,239 images with 5,041 instances of 46 aquatic animal species. We have also devised a simple yet effective multimodal-based scene-aware segmentation (MSAS) framework for segmenting aquatic animals at the instance level. In this framework, the results of multiple single-view segmentation models are fused under the guidance of a mask-independent controller. To overcome the problem of limited training data, we developed a guided mixup augmentation method based on a confusion matrix aimed at improving training performance. We have also established the first comprehensive benchmark for aquatic animal segmentation. Extensive experiments on the newly constructed dataset demonstrated the superiority of our proposed method over state-of-the-art instance segmentation methods (see Fig. 1). The dataset, source code, and models will be released with the publication of our paper.

Our contributions are five-fold:

- We present a comprehensive study on aquatic animal segmentation, which is more complicated than general object segmentation. This is the first exploration of this task to the best of our knowledge.
- We present a new dataset for aquatic animal segmentation. Our newly constructed AAS dataset contains 4,239 images of 46 aquatic animal species, in which each image has 1.2 instances on average. All images have instance-wise ground truths of bounding box and segmentation mask of aquatic animals.
- We propose a new multimodal-based scene-aware segmentation framework for aquatic animal segmentation. Our MSAS framework leverages different instance segmentation models by using multi-view mask fusion under the guidance of a mask-independent controller.
- We develop a new guided mixup augmentation method for improving segmentation performance. Our augmentation strategy boosts the performance of deep learning models from a discriminative ability perspective and maintains global context, especially for camouflaged animal.
- We introduce a comprehensive AAS benchmark to support advancements in this field.

2 Related Work

2.1 Instance Segmentation

Instance segmentation methods not only localize objects but also predict per-pixel segmentation masks of objects with their corresponding semantic labels. Pioneer methods [8–10] perform detect-then-segment by adding segmentation branches on top of Faster RCNN. More recent efforts have explored instance segmentation using ideas from other computer vision and graphics branches [11–14]. The use of different normalization layers has been proposed for reducing gradient vanishing to improve training performance [15, 16].

Along with those single instance segmentation methods, the fusion of several single segmentation models also plays an important role. Under circumstances when real-time inference is not required, ensemble modeling can improve robustness and effectiveness. Several techniques have been introduced for the object detection task that combine the predictions of multiple models and obtain a final set of detections. They include non-maximum suppression [17] and weighted boxes fusion [18]. To our best knowledge, a fusion technique for the instance segmentation task has not been developed. Here, we present a novel fusion algorithm leveraging a simple detector that performs as a view controller to ensemble predictions of single instance segmentation models.

2.2 Data Augmentation

Data augmentation consists of a collection of techniques that inflate the size and quality of training datasets used to improve the generalization ability of deep learning models [19]. Through augmentation, deep learning models are able to extract additional information from a dataset by data warping and/or oversampling. Data warping augmentation methods, which include geometric and color transformations, are always used in training deep learning models. Oversampling augmentation methods [20, 21] synthesize objects and then integrate them into the original training dataset. In addition, recent object-aware aug-

Table 1: Statistics for animal image datasets used in our experiments.

Dataset	#Cat.	#Train Img.	#Test Img.	#Img. per Cat.
MAS [25]	37	1,488	1,007	67.4
COD (Subset) [26]	21	758	293	50.0
CAMO++ (Subset) [27]	32	366	166	16.6
Proposed AAS	46	2,582	1,657	92.2

mentation methods [22, 23] aim to copy objects from an image and paste them into another image.

Our proposed AAS dataset contains images of aquatic animals, both camouflaged and non-camouflaged animals. The localization and recognition of an animal are much more complex and strongly depend on the entire background. This means that simply placing a cloned camouflaged animal on a random background is not working because within different contexts of scenes, the camouflaged animal becomes far easier to be recognized [24]. Our proposed guided mixup augmentation method overcomes this limitation better than existing augmentation methods for three reasons. (1) Rather than two images being randomly chosen and blended, a confusion matrix is leveraged with the aim of guiding the model to concentrate on misclassified categories. (2) The augmentation strategy helps instance segmentation models improve their discriminative ability by putting instances belonging to strongly confused categories into an image. (3) The use of mixup augmentation helps preserve the global context for both camouflaged and non-camouflaged animals.

3 Proposed Method

3.1 Aquatic Animal Species Dataset

To the best of our knowledge, only three currently available animal-image datasets can be used for aquatic animal segmentation: subsets of the MAS [25], COD [26], and CAMO++ [27] datasets. However, these datasets have different ranges of categories and a small number of images. This may lead to overfitting when training deep learning networks due to the small number of images in each category (see Table 1).

Our goal is to build a comprehensive benchmark that can be used to evaluate deep learning models. To reach this goal, we reorganized our AAS dataset by sampling the three datasets noted above and re-labeling the sampled

images. We first selected images containing aquatic animals from these datasets. Next, we manually discarded duplicate selected images and relabeled the images retained to match the categories in our dataset. Our reorganized dataset contains 4, 239 images of aquatic animals in 46 categories. There are 5, 041 instances in our dataset, and each image has 1.2 instances on average and a maximum of 22. Table 1 shows the overall statistics for our AAS dataset compared with the same three datasets.

3.2 Multimodal-based Scene-Aware Segmentation Framework

3.2.1 Overview

Instance segmentation methods [8, 10] are imperfect in the sense that each method may have advantages in specific contexts but disadvantages in others. To utilize the strength of each instance segmentation method, we derived a simple yet efficient **Multimodal-based Scene-Aware Segmentation (MSAS)** framework to leverage various models through mining image contexts.

Figure 2 illustrates our proposed MSAS framework, which consists of a training stage and an inference stage. In the training stage, instance segmentation models, dubbed “single-view models,” and a detection model, dubbed the “view controller,” are trained separately. The single-view models exploit different contexts to create different segmentation masks for the aquatic animals in the image. The view controller is aimed at producing pseudo bounding box ground truths for fusing multiple single-view models (see Section 3.2.2). In the inference stage, given an unlabeled image, the view controller extracts bounding boxes with high confidence scores from each image. These boxes guide the view controller as it fuses the results from the single-view models, resulting in the final segmentation mask results.

3.2.2 Multi-View Fusion

Our proposed multi-view mask fusion algorithm uses a mask-independent detector as the guidance view controller. The YOLOv5 [28]) model is used as the view controller thanks to its fast training and focusing for both spatial and discriminative representation.

Algorithm 1 illustrates our proposed multi-view fusion algorithm, which receives pseudo bounding box ground

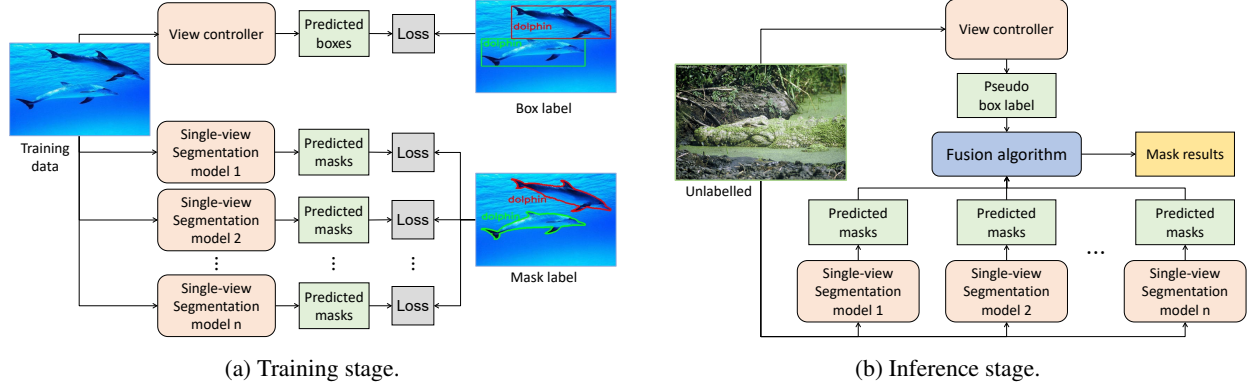


Figure 2: Workflow of multimodal-based scene-aware segmentation method (best viewed online in color with zoom).

truths and segmentation masks from single-view models as input and generates final mask results. It iterates over the images to update a “waiting list.” At each iteration, the segmentation masks of the single-view models for an image are added to the waiting list, and evaluation is performed to choose the best results.

In particular, when the algorithm is working with the i^{th} image, the “result list” contains the segmentation masks for the first $i - 1$ images. The waiting list is the union of the result list and a temporary segmentation mask for the i^{th} image. The average precision (AP) between the pseudo ground truths and the waiting list is then evaluated. If the n^{th} segmentation model provides the highest AP value, its segmentation mask for the i^{th} image is appended to the result list.

3.3 Guided Mixup Augmentation

Aquatic animals involve both camouflaged and non-camouflaged ones, which can confuse deep learning models. To address this problem, we developed a training procedure using guided mixup augmentation for instance segmentation. Different from the original mixup [20], which chooses random pairs of images for blending, our wisely guided mixing strategy chooses images using a confusion matrix. Figure 3 illustrates the workflow of our proposed guided mixup augmentation, which involves two stages: warmup learning and augmentation learning.

The first few steps are for warmup learning: the single-view model (*i.e.*, the instance segmentation model) tries to learn and adapt to new data by learning from only orig-

Algorithm 1 Multi-view fusion algorithm.

Input:

1. Collection of instance segmentation results $ins[M \times N]$ for N single-view models on M images.
2. List of pseudo ground truths $pseudo_{box}[M]$ for M images from view controller.

Output: List of results $res[M]$ for M images. Each element of ins , res contains all segmented results of corresponding image.

- 1: $res \leftarrow \emptyset$
 - 2: **for** $i \leftarrow 1$ to M **do**
 - 3: $\hat{n} \leftarrow \underset{n \in N}{\operatorname{argmax}}(\mathbf{AP}(pseudo_{box}[1 : i], res \cup ins[i, n]))$
 - 4: $res \leftarrow res \cup ins[i, \hat{n}]$
 - 5: **return** res
-

inal images. Therefore, augmentation is not used in these initial learning steps.

Next, in the augmentation learning stage, when the single-view model achieves stable weights at the end of each epoch, a confusion matrix is constructed on the basis of the bounding box IoU (intersection over union) between the segmentation results and ground truths. For each segmented instance, all instance ground truths having an IoU with the segmented instance mask larger than threshold $\alpha = 0.5$ are selected. The category and classification score for all matching pairs of results and ground truths are extracted and used to create guided confusion

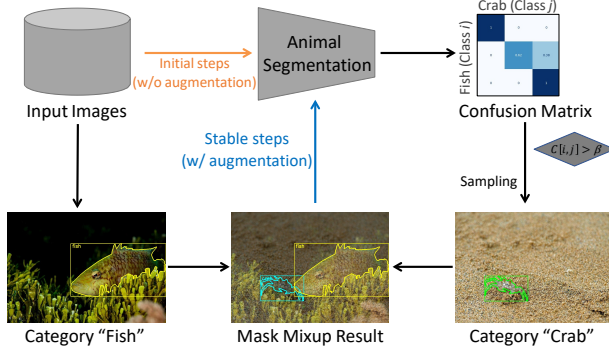


Figure 3: Workflow of proposed guided mixup augmentation using confusion matrix (best viewed online in color with zoom).

matrix (C) for the next epoch.

In the next epoch, given an input image, we select an ambiguous image from the training set for mixing. In particular, for pairs of strongly misclassified categories (i, j) (i.e., $C[i][j]$ is larger than threshold $\beta = 0.2$), if the input image contain instances of category i , a random image having instances in category j is selected from the training set.

Given two images a and b with resolutions (H_1, W_1) and (H_2, W_2) , the images are resized to $(\frac{H_1+H_2}{2}, \frac{W_1+W_2}{2})$ and then mixed together using $c = \gamma \times \phi(a) + (1 - \gamma) \times \phi(b)$, where $\phi(\cdot)$ denotes random cropping and translation operations. Output image c contains all instances in both original images along with their ambiguous categories. Standard transformations, such as color jitter, brightness adjustment, and horizontal flipping, are applied to the output image. We empirically set $\gamma = 0.5$.

4 Experiments

4.1 Implementation

We used ten instance segmentation models as the single-view models in our proposed MSAS framework: Mask RCNN [8], Cascade Mask RCNN [9], GN-Mask RCNN [15], Mask Scoring RCNN [10], Deformable ConvNets [12], GCNet [13], CARAFE [11], WS-Mask RCNN [16], PointRend [14], and GRoIE [29]. All of

Table 2: Average precisions of state-of-the-art instance segmentation methods and proposed method; 1st and 2nd places are shown in **blue** and **red**, respectively.

Method	AP	AP50	AP75
Mask RCNN [8]	15.6	24.3	15.8
Cascade Mask RCNN [9]	20.6	30.2	22.2
GN-Mask RCNN [15]	15.5	23.2	16.3
Mask Scoring RCNN [10]	17.3	27.1	18.1
Deformable ConvNets [12]	16.0	24.0	17.4
GCNet [13]	12.1	18.7	13.0
CARAFE [11]	14.7	22.7	15.2
WS-Mask RCNN [16]	18.7	27.1	20.7
PointRend [14]	12.7	18.7	13.3
GRoIE [29]	17.8	26.8	18.9
MSAS w/o augmentation	24.9	36.3	26.5
MSAS with augmentation	28.3	40.7	31.4

them were used with the widely used ResNet50-FPN backbone. A YOLOv5 [28] detector was used as the view controller.

All models were trained with a batch size of 2 on an RTX 2080Ti GPU. They were fine-tuned from their publicly released MS-COCO pre-trained models. The single-view segmentation models were trained using stochastic gradient descent optimization with a weight decay of 10^{-4} and momentum of 0.9. The first 500 steps were used for warmup learning, in which the learning rate was set to 2×10^{-5} and then linearly increased to 0.02. The models were then trained for 12 epochs with a base learning rate of 0.02, which was decreased by 10 times at the 8th and 11th epochs. Data augmentation was not applied in the first epoch so that the models could adapt to the aquatic animal images. From the second epoch, our proposed guided mixup data augmentation method was applied. The ratio of augmented images and original images was kept at 50/50 by using a Bernoulli distribution. The view controller was trained for 500 epochs with an image size of 1280×1280 and data augmentation.

4.2 Comparison with State-of-the-art Methods

In this section, we compare our MSAS framework with state-of-the-art methods to demonstrate the superiority of the proposed method. Table 2 shows the performance of



Figure 4: Comparison of results from different methods. From left to right: input images, followed by overlaid ground truths, and results of our MSAS framework, Mask RCNN [8], Cascade Mask RCNN [9], MS RCNN [10], PointRend [14], WS-Mask RCNN [16], GRoIE [29]. Instances shown in color differ from the ground truth denote misclassification.

different methods in terms of Average Precision (AP). As can be seen, our proposed method, MSAS, achieved the best performance in all metrics. Even training on only original images without data augmentation, our method still surpassed the state-of-the-art methods by a remarkable margin in all metrics. Meanwhile, the completed MSAS framework significantly outperformed all compared methods in all metrics. It shows the effectiveness of the proposed guided mixup augmentation, which results in an impressive increase of 3.4 in AP.

Comparison of the performance of our multimodal-based scene-aware segmentation method with those of state-of-the-art methods demonstrated its superiority. As shown in Table 2, our proposed method achieved the best performance for all three AP metrics. Even when trained on only original images without data augmentation, our method still surpassed the state-of-the-art methods by a remarkable margin on all metrics. The complete MSAS

framework with data augmentation significantly outperformed all compared methods on all metrics and showed an impressive 3.4 increase in AP over the MSAS framework without data augmentation. These results demonstrate the effectiveness of the proposed guided mixup augmentation method.

Figure 4 shows a visual comparison of the tested methods. The MSAS framework achieved the best results, and the results are close to the ground truth. Our method effectively handled both segmentation mask and classification label.

4.3 Ablation Studies

We also investigated the efficiency of our proposed MSAS framework through an ablation study. In particular, we took into account the number of single-view models and the effectiveness of guided mixup augmentation.

Table 3: Effectiveness of data augmentation. Best results are shown in **blue**.

Method	AP	AP50	AP75
None	21.7	32.5	22.5
Random mixup [20]	21.2	31.4	22.7
Instaboost [22]	21.5	31.7	23.9
Copy-paste [23]	22.8	34.0	24.2
Guided mixup	23.8	34.5	26.7

4.3.1 Number of Single-View Models

We investigated the effectiveness of our multi-view fusion by increasing the number of single-view models one by one. To show the actual contribution of the proposed fusion algorithm, we did not use our guided mixup data augmentation to train the models. As shown in Fig. 5, the accuracy of the MSAS framework plateaued at ten models. Further increases in the number of single-view models would only lead to increasing processing time without improving performance. Hence, we use ten single-view models in our MSAS framework.

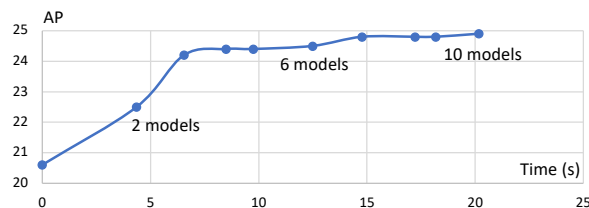


Figure 5: Trade-off between accuracy and processing time as number of single-view models was increased. Accuracy plateaued at ten models.

4.3.2 Guided Mixup Augmentation

We demonstrated the usefulness of our proposed guided mixup augmentation method, with its category discrimination ability, by comparing its performance with that of three data augmentation methods: random mixup [20], instaboost [22], and copy-paste [23]. Table 3 shows the performance of our MSAS framework using a simple version with two single-view models (Mask RCNN and Cascade Mask RCNN), trained using different data augmentation methods. Our guided mixup augmentation method sub-

stantially improved the performance of the MSAS framework without data augmentation by 9.7%. The performance of the proposed data augmentation method also surpassed that of existing data augmentation methods by a remarkable margin. Hence, our proposed wisely guided augmentation method will make a strong contribution not only to reducing data labeling hours but also to efficiency (*i.e.*, processing time) and effectiveness (*i.e.*, performance improvement).

5 Conclusion

We investigated the interesting yet challenging problem of aquatic animal segmentation and created the Aquatic Animal Species (AAS) dataset containing images of diverse aquatic animal species. Each image has an annotated instance-level mask ground truth. We also developed a novel multimodal-based scene-aware segmentation framework that uses a multi-view fusion algorithm to leverage different instance segmentation models. We further boosted the performance of aquatic animal segmentation by developing a guided mixup augmentation method. Extensive experiments demonstrated that our proposed method achieves state-of-the-art performance on our newly constructed dataset. We expect that our AAS dataset will greatly support research activities related to automatically identifying new aquatic animal species.

Acknowledgements

This work was funded by Gia Lam Urban Development and Investment Company Limited, Vingroup and supported by Vingroup Innovation Foundation (VINIF) under project code VINIF.2019.DA19., National Science Foundation Grant (NSF#2025234), JSPS KAKENHI Grants (JP16H06302, JP18H04120, JP21H04907, JP20K23355, JP21K18023), and JST CREST Grants (JPMJCR20D3, JPMJCR18A6). We gratefully acknowledge NVIDIA for their support of the GPUs.

References

- [1] Li Liu, Wanli Ouyang, Xiaogang Wang, Paul W. Fieguth, Jie Chen, Xinwang Liu, and Matti Pietikäinen, “Deep learning for generic object detection: A survey,” *IJCV*, vol. 128, 2019.

- [2] Shervin Minaee, Yuri Y. Boykov, Fatih Porikli, Antonio J Plaza, Nasser Kehtarnavaz, and Demetri Terzopoulos, "Image segmentation using deep learning: A survey," *IEEE TPAMI*, 2021.
- [3] Mackenzie Weygandt Mathis and Alexander Mathis, "Deep learning tools for the measurement of animal behavior in neuroscience," *Current Opinion in Neurobiology*, vol. 60, pp. 1–11, 2020, Neurobiology of Behavior.
- [4] Takuya Maekawa, Kazuya Ohara, Yizhe Zhang, Matasaburo Fukutomi, Sakiko Matsumoto, Kentarou Matsumura, Hisashi Shidara, Shuhei J. Yamazaki, Ryusuke Fujisawa, Kaoru Ide, Naohisa Nagaya, Koji Yamazaki, Shinsuke Koike, Takahisa Miyatake, Koutarou D. Kimura, Hiroto Ogawa, Susumu Takahashi, and Ken Yoda, "Deep learning-assisted comparative analysis of animal trajectories with deepl," *Nature Communications*, vol. 11, 2020.
- [5] Omkar M. Parkhi, Andrea Vedaldi, Andrew Zisserman, and C. V. Jawahar, "Cats and dogs," in *CVPR*, 2012.
- [6] C. Wah, S. Branson, P. Welinder, P. Perona, and S. Belongie, "The Caltech-UCSD Birds-200-2011 dataset," Tech. Rep. CNS-TR-2011-001, California Institute of Technology, 2011.
- [7] Xiaoping Wu, Chi Zhan, Yukun Lai, Ming-Ming Cheng, and Jufeng Yang, "IP102: A large-scale benchmark dataset for insect pest recognition," in *CVPR*, 2019.
- [8] Kaiming He, Georgia Gkioxari, Piotr Dollár, and Ross Girshick, "Mask r-cnn," in *ICCV*, 2017.
- [9] Zhaowei Cai and Nuno Vasconcelos, "Cascade r-cnn: Delving into high quality object detection," in *CVPR*, 2018.
- [10] Zhaojin Huang, Lichao Huang, Yongchao Gong, Chang Huang, and Xinggang Wang, "Mask Scoring R-CNN," in *CVPR*, 2019.
- [11] Jiaqi Wang, Kai Chen, Rui Xu, Ziwei Liu, Chen Change Loy, and Dahua Lin, "Carafe: Content-aware reassembly of features," in *ICCV*, October 2019.
- [12] Xizhou Zhu, Han Hu, S. Lin, and Jifeng Dai, "Deformable convnets v2: More deformable, better results," *CVPR*, 2019.
- [13] Yue Cao, Jiarui Xu, Stephen Lin, Fangyun Wei, and Han Hu, "Gcnet: Non-local networks meet squeeze-excitation networks and beyond," in *ICCV Workshop*, 2019.
- [14] Alexander Kirillov, Yuxin Wu, Kaiming He, and Ross Girshick, "Pointrend: Image segmentation as rendering," in *CVPR*, June 2020.
- [15] Yuxin Wu and Kaiming He, "Group normalization," in *ECCV*, 2018.
- [16] Siyuan Qiao, Huiyu Wang, Chenxi Liu, Wei Shen, and Alan Yuille, "Weight standardization," *arXiv preprint arXiv:1903.10520*, 2019.
- [17] N. Dalal and B. Triggs, "Histograms of oriented gradients for human detection," in *CVPR*, 2005.
- [18] Roman Solovyev, Weimin Wang, and Tatiana Gabruseva, "Weighted boxes fusion: Ensembling boxes from different object detection models," *Image and Vision Computing*, vol. 107, pp. 104117, 2021.
- [19] Connor Shorten and T. Khoshgoftaar, "A survey on image data augmentation for deep learning," *Journal of Big Data*, vol. 6, 2019.
- [20] Hongyi Zhang, Moustapha Cisse, Yann N. Dauphin, and David Lopez-Paz, "mixup: Beyond empirical risk minimization," in *ICLR*, 2018.
- [21] Ian J. Goodfellow, Jean Pouget-Abadie, Mehdi Mirza, Bing Xu, David Warde-Farley, Sherjil Ozair, Aaron Courville, and Yoshua Bengio, "Generative adversarial nets," in *NeurIPS*, 2014, p. 2672–2680.
- [22] Hao-Shu Fang, Jianhua Sun, Runzhong Wang, Minghao Gou, Yong-Lu Li, and Cewu Lu, "Instaboost: Boosting instance segmentation via probability map guided copy-pasting," in *ICCV*, October 2019.
- [23] Golnaz Ghiasi, Yin Cui, Aravind Srinivas, Rui Qian, Tsung-Yi Lin, Ekin D. Cubuk, Quoc V. Le, and Barret Zoph, "Simple copy-paste is a strong data augmentation method for instance segmentation," in *CVPR*, June 2021, pp. 2918–2928.
- [24] Trung-Nghia Le, Tam V. Nguyen, Zhongliang Nie, Minh-Triet Tran, and Akihiro Sugimoto, "Anabran network for camouflaged object segmentation," *CVIU*, vol. 184, pp. 45–56, 2019.
- [25] Lin Li, Eric Rigall, Junyu Dong, and Geng Chen, "MAS3K: an open dataset for marine animal segmentation," in *BenchCouncil International Symposium on Benchmarking, Measuring, and Optimizing*, 2020, pp. 194–212.
- [26] Deng-Ping Fan, Ge-Peng Ji, Guolei Sun, Ming-Ming Cheng, Jianbing Shen, and Ling Shao, "Camouflaged object detection," in *CVPR*, 2020.
- [27] Trung-Nghia Le, Yubo Cao, Tan-Cong Nguyen, Minh-Quan Le, Khanh-Duy Nguyen, Thanh-Toan Do, Minh-Triet Tran, and Tam V. Nguyen, "Camouflaged instance segmentation in-the-wild: Dataset, method, and benchmark suite," *IEEE TIP*, 2021.
- [28] Glenn Jocher, K Nishimura, T Mineeva, and R Vilariño, "Yolov5," *Code repository <https://github.com/ultralytics/yolov5>*, 2020.
- [29] L. Rossi, Akbar Karimi, and A. Prati, "A novel region of interest extraction layer for instance segmentation," *ICPR*, 2021.